New Phytologist

Research

Root-associated fungal communities are influenced more by soils than by plant-host root traits in a Chinese tropical forest

J. Aaron Hogan[1,6], Michelle A. Jusino[2,3], Matthew E. Smith[2], Adriana Corrales[2,4], Xiaoyang Song[5], Yue-hua Hu[5], Jie Yang[5], Min Cao[5], Oscar J. Valverde-Barrantes[1] and Christopher Baraloto[1]

[1]Department of Biological Sciences, Institute of Environment, Florida International University, Miami, FL 33199, USA; [2]Department of Plant Pathology, University of Florida, Gainesville, FL 32611, USA; [3]USDA Forest Service, Northern Research Station, Center for Forest Mycology Research, Madison, WI 53726, USA; [4]Centro de Investigaciones en Microbiología y Biotecnología-UR (CIMBIUR), Facultad de Ciencias Naturales, Universidad del Rosario, Bogotá 111221, Colombia; [5]CAS Key Laboratory of Tropical Forest Ecology, Xishuangbanna Tropical Botanical Garden, Chinese Academy of Sciences, Yunnan 666303, China; [6]Present address: Department of Biology, University of Florida, Gainesville, FL 32611, USA

Author for correspondence:
J. Aaron Hogan
Email: hogan.jaaron@ufl.edu

Received: *12 November 2022*
Accepted: *14 February 2023*

New Phytologist (2023) **238:** 1849–1864
doi: 10.1111/nph.18821

Key words: fungal ITS2, mycorrhizas, root functional traits, root tissue chemistry, tropical trees, Xishuangbanna.

Summary

- Forest fungal communities are shaped by the interactions between host tree root systems and the associated soil conditions. We investigated how the soil environment, root morphological traits, and root chemistry influence root-inhabiting fungal communities in three tropical forest sites of varying successional status in Xishuangbanna, China.
- For 150 trees of 66 species, we measured root morphology and tissue chemistry. Tree species identity was confirmed by sequencing rbcL, and root-associated fungal (RAF) communities were determined using high-throughput ITS2 sequencing.
- Using distance-based redundancy analysis and hierarchical variation partitioning, we quantified the relative importance of two soil variables (site average total phosphorus and available phosphorus), four root traits (dry matter content, tissue density, specific tip abundance, and forks), and three root tissue elemental concentrations (nitrogen, calcium, and manganese) on RAF community dissimilarity. The root and soil environment collectively explained 23% of RAF compositional variation. Soil phosphorus explained 76% of that variation. Twenty fungal taxa differentiated RAF communities among the three sites.
- Soil phosphorus most strongly affects RAF assemblages in this tropical forest. Variation in root calcium and manganese concentrations and root morphology among tree hosts, principally an architectural trade-off between dense, highly branched vs less-dense, herringbone-type root systems, are important secondary determinants.

Introduction

Relationships between plant roots and their associated fungi range from parasitic to mutualistic (Smith & Read, 2008; van der Heijden *et al.*, 2015). The development of root systems was a significant evolutionary leap that led to land plant diversification (Kenrick & Strullu-Derrien, 2014; Strullu-Derrien *et al.*, 2016). Fungal colonization of root systems occurred concurrently with root system evolution, and the ability of plants to harbor fungi has been crucial to the radiation and dominance of terrestrial plant life over the last several geological eras (Brundrett, 2002). Nowhere are the consequences of such an intertwined evolutionary dance between plant roots and fungi more visible than in hyperdiverse tropical forests, where plant and fungal communities interact to strongly influence forest community and ecosystem processes (Lovelock & Ewel, 2005; Peay *et al.*, 2013; Sarmiento *et al.*, 2017; Corrales *et al.*, 2018; Reichert *et al.*, 2022).

Interactions between fungal function (e.g. nutrient and water acquisition) and plant hosts have shaped root form (e.g. root diameter and topology; Hetrick, 1991; McCormack & Iversen, 2019). For example, a fundamental axis of root functional trait variation, the root system fungal collaboration gradient (Bergmann *et al.*, 2020), describes a trade-off between thin diameter, long roots with thin root cortical areas that acquire nutrients primarily by themselves (e.g. without fungi) vs thicker, shorter roots, with more root cortical tissue that acquire nutrients primarily via mycorrhizal outsourcing (Chen *et al.*, 2016; Ma *et al.*, 2018; Bergmann *et al.*, 2020). Considering this trade-off, the entire length of absorptive roots (those $\leq$ 2 mm in diameter, Pregitzer *et al.*, 2002; McCormack *et al.*, 2015), especially root tips, can be considered distinct habitats that harbor separate assemblages of root symbionts. This is akin to how in metacommunity theory individual sites can harbor distinct assemblages of organisms that are subsets of the greater regional species pool (Leibold *et al.*, 2004; Leibold & Chase, 2018). Within this framework, and because root-associated fungi (RAF) are mostly dispersal-limited (Peay *et al.*, 2010a,b), soils and roots can be viewed as successive

environmental filters that shape RAF assemblages (Jumpponen & Egerton-Warburton, 2005).

Separating how environmental filtering and host identity affect RAF communities has proven difficult. For example, in the western Amazon, soil type (e.g. terra firme vs white sands) is a principal driver of fungal community composition (Peay *et al.*, 2013), with soil pH and carbon affecting local-scale fungal β-diversity (Vasco-Palacios *et al.*, 2020). Soil type also drives the environmental filtering of tree communities from the regional species pool (Fine & Kembel, 2011; Baraloto *et al.*, 2021), which affects associations between plant roots and the soil environment. Furthermore, fungal and tree diversity are correlated across gradients in soil type, pointing to intricate linkages between the soil environment, the plant community composition, and putatively plant–fungal interactions (Peay *et al.*, 2013; Reichert *et al.*, 2022). Other studies have shown that the soil environment in tropical forests has a strong effect on tree–fungal community associations (Gourmelon *et al.*, 2016; Essene *et al.*, 2017; Weemstra *et al.*, 2020).

However, the degree to which root functional (i.e. morphological and chemical) traits influence RAF communities in natural tropical forests is not well documented. Most of the studies that evaluate how root morphology and RAF communities covary with variation in soil habitat often do so superficially. For instance, most studies either classify plant-host taxa generally as ectomycorrhizal (ECM) vs arbuscular mycorrhizal (AM; e.g. Weemstra *et al.*, 2020; Ferlian *et al.*, 2021) or use indirect measures of root functional traits from trait databases rather than via direct measurements (e.g. McCormack & Iversen, 2019). Thus, there is a need to directly measure and characterize root functional traits and root-inhabiting fungal communities across edaphic gradients to elucidate the role root functional strategies play in determining assemblages of fungal symbionts (Fei *et al.*, 2022).

We aimed at linking root functional traits to their root-inhabiting fungal communities at the root system level for tropical forest trees in southwest China. We measured root morphology, chemistry, and fungal assemblages of intact root systems (3–4 root orders) and related them to site-level soil measurements for three forest sites of varying forest age and tree composition to address two key questions. First, what are the relative strengths of root functional traits, root chemistry, and the soil environment in determining RAF composition? Some recent molecular studies in tropical forests have shown that soils impact RAF community composition more than plant hosts (Essene *et al.*, 2017; Maciá-Vicente *et al.*, 2020; Weemstra *et al.*, 2020). We therefore anticipated strong effects of the soil environment, outweighing the effects of tree species and their root functional traits. However, we expected distinct assemblages among AM and ECM hosts, which should relate to functional (e.g. construction cost) tradeoffs in root morphology (i.e. root system topology or root tissue density – RTD) (Kong *et al.*, 2019). We expected relationships of RAF assemblages, root functional traits, and the soil environment to be variable and depend on soil fertility and the prevalence and host specificity of beneficial (e.g. symbiotrophic) fungi and nonbeneficial (e.g. saprotrophic and pathogenic) fungi. Second, what fungal taxa and functional guilds drive differentiation in community composition? Tree root system associations with AM and saprotrophic fungi dominate tropical forests, especially in older, well-developed stands (Janos, 1980; Muthukumar *et al.*, 2003a; Alexander & Lee, 2005), but ECM tree roots present unique fungal niches and are an important component of some tropical forests (Corrales *et al.*, 2018). If soils are the main driver of RAF community dissimilarity, then site differences should supersede root functional trait effects or differences in root-host affinity for AM vs ECM interactions.

Materials and Methods

Study sites

We sampled trees from three sites in the Xishuangbanna tropical forest region of southwestern China. We selected three Chinese Ecological Research Network (CERN) sites near Xishuangbanna Tropical Botanical Garden (XTBG) with varying successional states and differences in soil conditions. The first site (0.5-ha plot) was a 60-yr-old secondary forest adjacent to a rubber plantation within the grounds of the XTBG ('secondary near rubber plantation', SR). The other two sites were in a nearby conservation area: a 0.5-ha plot of 60-yr-old secondary forest ('secondary evergreen', SE), and a 1-ha plot in a primary, old-growth forest with no history of past disturbance ('rainforest', RF; see Supporting Information Methods S1 for additional site details).

Soil measurements

We characterized the soil environments of each of the three sites using data from previous CERN soil sampling (Pan *et al.*, 2019, Methods S2). We used site averages of soil nutrients in our analyses ($n = 72$ per site) because there were no records of spatial locations of soil samples relative to the coordinates of trees at each site. Although averages obscure variability among habitats within sites, they generally represent landscape-scale variation in soil fertility among sites (Pan *et al.*, 2019). Thus, the average soil conditions can be viewed as a higher-order environmental filter affecting root-inhabiting fungal communities (Jumpponen & Egerton-Warburton, 2005). We conducted a principal components analysis (PCA) of soil variables and tested for statistical differences in soil variables among sites using one-way ANOVA with Tukey HSD *post hoc* comparisons.

Root system functional traits and tissue chemistry

Root systems were collected from previously tagged and identified individual trees within plots (see Methods S3). We targeted trees of known taxonomic identity from 18 families (Anacardiaceae, Annonaceae, Burseraceae, Clusiaceae, Ebenaceae, Euphorbiaceae, Fagaceae, Juglandaceae, Lauraceae, Lecythidaceae, Moraceae, Myrsticaceae, Myrsinaceae, Pittosporaceae, Polygalaceae, Rutaceae, Sapindaceae, and Ulmaceae). We selected these families because they are common in this forest and represent the main clades across the Angiosperm phylogeny, maximizing the range of variation in

root functional traits (Valverde-Barrantes *et al.*, 2017). Intact root systems were processed using common protocols for measuring root functional traits and tissue elemental concentrations (see Methods S3; Fig. S1; McCormack *et al.*, 2015).

Sequencing of root fungal communities

Root tips were preserved in a lysis solution containing 2% CTAB and were frozen until processed. DNA extractions were done using the protocol detailed in Lindner & Banik (2009) with modifications in Brazee & Lindner (2013; see Methods S4; Fig. S2). The fungal ITS2 (nuclear ribosomal Internal Transcribed Spacer 2) region was amplified using a primer mixture that consisted of equal parts fITS7 (Ihrmark *et al.*, 2012) and fITS7o forward primers (Kohout *et al.*, 2014) and ITS4 reverse primer (White *et al.*, 1990; see Table S1). This primer combination can amplify both AM and ECM fungi (Lekberg *et al.*, 2018). Primers were appended with Illumina Nextera adapters. Polymerase chain reaction (PCR) was used to amplify the fungal ITS2 region (Methods S4). Nextera indices were applied in a second 8-cycle PCR. Negative extraction, PCR, and indexing controls were included and carried through each downstream step. Our positive sequencing control was a single-copy, nonbiological synthetic mock community (SynMo; Palmer *et al.*, 2018). Indexed amplicons were cleaned using a SequalPrep Normalization Plate Kit (ThermoFisher Scientific, Waltham, MA, USA) and pooled, and the combined library underwent a final bead clean-up. Sequencing was done on an Illumina MiSeq (2 × 300 bp reads, v3 chemistry) at the University of Florida Interdisciplinary Center for Biotechnology Research.

Sequences were processed using AMPtk (Palmer *et al.*, 2018). Forward and reverse reads were demultiplexed, merged, and quality-checked. Poor-quality reads were discarded, sequences were dereplicated, and operational taxonomic units (OTUs) were assigned via clustering, using a 97% identity threshold. Sequences were then chimera-filtered and mapped to OTUs. SynMo was used to identify and correct index bleed and to parameterize our bioinformatic processing (Palmer *et al.*, 2018). Finally, OTUs were assigned taxonomy using the hybrid taxonomy method in AMPtk, which calculates a consensus last common ancestor taxonomy based on the results of Global Alignment (USEARCH/VSEARCH), UTAX, and SINTAX databases. Fungal guilds were assigned using the FUNGuild database (Nguyen *et al.*, 2016). Although we used all guild classification data returned by FUNGuild (including possible and probable confidence rankings), we combined the 101 returned guild classifications into 11 broad fungal trophic guilds, which we have high confidence in (see Methods S5).

Sequencing of plant DNA

To verify the taxonomic identity of plant roots, we sequenced the coding region of the rbcL chloroplast marker in all samples for which we sequenced fungal ITS2 (Kress & Erickson, 2007; Table S1). Sanger sequences were blasted against rbcL sequences from the XTBG tree community (X. C. Huang *et al.*, 2015; GenBank accession nos. KR528589–KR534171), using a 98% similarity threshold. We chose rbcL because X. C. Huang *et al.* (2015) found that rbcL was the most easily amplified marker that provided genus-level identification. Therefore, we limited subsequent analyses to samples where rbcL sequences matched the genus of field identification, leaving a dataset of 150 trees from 66 species comprising 18 families. Twelve of the 66 tree species (members of the Fagaceae and Juglandaceae) host ECM fungi, whereas the remainder harbor AM fungi. Six ECM trees were sampled in RF (1% of trees sampled in that plot) and six ECM trees were sampled in SR (14%), whereas 19 ECM trees were sampled in SE (41%).

Statistical analyses – forward selection of variables

All statistical analyses were carried out in R v.4.0.5 (R Core Team, 2021). We chose forward selection (Blanchet *et al.*, 2008) to reduce the number of variables to a manageable set (see Methods S6). The procedure identified nine environmental parameters that are most related to fungal community dissimilarities (Table S2), including two soil variables (average available and total soil P), four root functional traits (root dry matter content: RDMC, specific root tip abundance: SRTA, number of root forks, and RTD), and three root tissue elemental concentrations (root N, Ca, and Mn). Collectively, these variables explained 18% of RAF community dissimilarity (Table S2). Coefficients of determination from forward selection were 0.07 for soil available P and 0.05 for soil total P. The four forward-selected root functional traits were all similar in strength with coefficients of determination near 0.01. Root tissue elemental concentrations all had coefficients of determination < 0.01 (Table S2).

Statistical analyses – root functional traits, fungal richness, diversity, and evenness

We compared the forward-selected root functional traits and tissue chemistry concentrations from 450 root systems of 150 individual trees using a single-factor ANOVA, followed by a Tukey HSD *post hoc* comparison among sites. For each RAF community (by individual tree), we computed species richness, Shannon's diversity (H'; Shannon, 1948), and Pielou's species evenness (J'; Pileou, 1966). Analyses of variance, followed by Tukey HSD *post hoc* comparisons, were conducted to compare richness, diversity, and evenness across sites. We used ordinary least-squares regressions to analyze relationships between the nine forward-selected environmental variables (soil available P, soil total P, RDMC, SRTA, root system forks, RTD, root N, root Ca, and root Mn) and H', richness and J'.

Statistical analyses – distance-based redundancy analyses, hierarchical variation partitioning, and generalized additive models

To examine the relative influence of root functional traits, root tissue chemistry, and soil nutrient status on RAF community composition, we used multivariate distance-based redundancy

analysis (db-RDA; Ter Braak, 1994; Legendre & Anderson, 1999; Legendre & Legendre, 2012). The db-RDA was implemented using the 'capscale' function of the VEGAN package (Oksanen *et al.*, 2020), with fungal ITS2 presence–absence and the Sørensen distance measure (Sørensen, 1948). The nine forward-selected environmental variables were *z*-score transformed before the analysis. The db-RDA was statistically evaluated using ANOVA, where we tested the significance of the entire model, each of the constrained ordination axes, and the terms of the model separately. Next, we used an extension of variation partitioning (Peres-Neto *et al.*, 2006; Legendre & Legendre, 2012) called hierarchical partitioning, which allows for the variation partitioning of more than three predictor variables (or sets of predictor variables, Lai *et al.*, 2021; see Methods S7). The procedure quantified the contribution of each environmental predictor to the db-RDA.

To directly assess the nature of how each forward-selected environmental variable was related to RAF-community dissimilarity, we used generalized additive models (GAMs, see Methods S7). We fit GAMs using the 'ordisurf' function in the VEGAN package (Oksanen *et al.*, 2020), which employs 'gam' from the MCGV package and estimates the smoothness of model terms when fitting (Wood, 2011). The significance of the linear term is tested with a *t*-test, whereas smooth terms are tested with *F*-tests. To visualize GAM fits, we plotted model surface contours onto the constrained ordination space.

Statistical analyses – similarity percentages for discriminating taxa

To identify which fungal taxa were driving community dissimilarity among sites (i.e. discriminating taxa), we calculated the similarity percentages among sites (i.e. SIMPER, Clarke, 1993). Because site effects typically outweighed tree species (i.e. root functional trait) effects in determining fungal community composition, we used site groupings rather than root species identity. The SIMPER procedure calculates the average contribution of each fungal species to the average pairwise dissimilarity among sites and then identifies the taxa which account for ≥ 70% of site compositional differences for each pairwise comparison. We first removed OTUs that contributed < 1% of total reads and used 9999 permutations. To test the significance of SIMPER-identified OTUs, we used the nonparametric Kruskal–Wallis rank-sum test for each pairwise comparison. We adjusted *P*-values from the Kruskal–Wallis test for false discovery rate (Benjamini & Hochberg, 1995). Sequences identified in the SIMPER analysis were blasted against the UNITE database to confirm fungal taxonomy, trophic mode, and guild (Nilsson *et al.*, 2018).

Results

Soil environmental variation

The soil conditions of the three sites varied (Fig. 1). PCA axis 1 explained 47.3% of the variation in soil variables and was directly related to total soil N; PCA axis 2 explained 19.3% of the variation in soils and best related to total soil K (Fig. 1). Soil nutrient concentrations differed significantly among sites for all seven variables (Table 1, $F_{(2,213)} = 25.87–84.18$, all $P < 0.001$). Tukey HSD groups were distinct among all three sites for soil organic matter (greatest in SR), total N (greatest in SR), and available P (greatest in RF). Tukey HSD groups for soil pH showed SR had slightly more acidic soils than the other two sites. SR also had more available and total P than the other two sites. SE had less total P than SR or RF, which were not statistically different from each other (Table 1).

Root functional trait and tissue chemistry

Within sites, despite attempting to control for tree host identity, representative samples of tree root functional traits differed. Four of the seven forward-selected traits (RDMC, Forks, STRA, and root Ca) differed significantly among sites, one trait (RTD) was marginally different, and two traits (root N and Mn) were not statistically different (Table 2). RDMC in SR was less than RDMC in the other two sites. The number of root system forks was greater in SE than in RF but was not significantly different between SR and either RF or SE (Table 2). RTD was lower in the SE than in the other two sites. SRTA was greater in RF and SE than in SR. Lastly, root Ca was greatest in RF, but root N and Mn were not statistically different across sites (Table 2). The four forward-selected root functional traits characterize the root architectural space (i.e. along PCA axis 1, Fig. S3A), with variable contributions to the first three axes (Table S3). The three forward-selected root tissue elements were arranged at varying

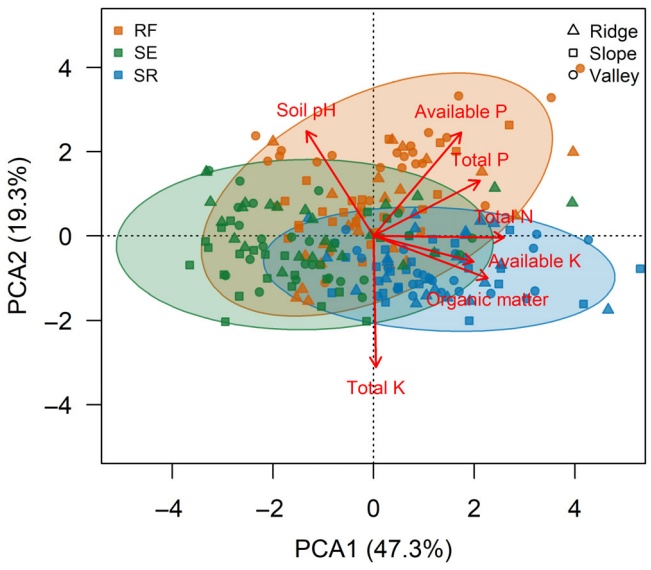

Fig. 1 Principal components biplot of the first two principal components (PC) axes using seven soil variables measured on ridge, slope, and valley habitats on each of the three study plots (RF, primary rainforest; SE, secondary evergreen; SR, secondary near rubber plantation). Study plots were located near the Xishuangbanna Tropical Botanical Garden in Menglun, Mengla, Yunnan, China. Soil samples ($n = 72$ per plot) were collected in 2010 and 2015 randomly across plots by habitat (ridge, slope, and valley). Colors represent each plot, while shapes represent habitats. Ellipses show 95% confidence interval limits.

Table 1 Mean (±SE) soil properties for the three study plots near the Xishuangbanna Tropical Botanical Garden in Menglun, Mengla, Yunnan, China.

Plot	Soil pH	Organic matter (g kg^{-1})	Total N (g kg^{-1})	Total P (g kg^{-1})	Total K (g kg^{-1})	Available P (mg kg^{-1})	Available K (mg kg^{-1})
Primary rainforest (RF)	4.41 ± 0.02^{b}	30.77 ± 0.76^{a}	1.99 ± 0.04^{b}	0.35 ± 0.01^{b}	8.42 ± 0.01^{a}	3.77 ± 0.17^{c}	66.36 ± 2.32^{a}
Secondary evergreen (SE)	4.42 ± 0.02^{b}	34.20 ± 0.97^{b}	1.60 ± 0.04^{a}	0.22 ± 0.01^{a}	8.61 ± 0.02^{a}	1.84 ± 0.12^{a}	62.17 ± 2.58^{a}
Secondary near rubber plantation (SR)	4.26 ± 0.02^{a}	41.95 ± 0.92^{c}	2.34 ± 0.04^{c}	0.33 ± 0.01^{b}	9.53 ± 0.01^{b}	2.78 ± 0.11^{b}	87.57 ± 3.07^{b}
F-statistic	$F_{(2,213)} = 26.25$	$F_{(2,213)} = 41.83$	$F_{(2,213)} = 76.45$	$F_{(2,213)} = 84.18$	$F_{(2,213)} = 20.27$	$F_{(2,213)} = 51.12$	$F_{(2,213)} = 25.87$
P	***	***	***	***	***	***	***

ANOVA statistics are given with associated probabilities. Letters denote *post hoc* Tukey HSD test groupings. *P*-values are denoted as follows: ns, nonsignificant $P > 0.1$; *, $P < 0.05$; **, $P < 0.01$; ***, $P < 0.001$.

Table 2 Average fine root system functional trait values and tissue elemental concentrations for 450 root systems of 150 individual trees collected across three small forest dynamics plots near the Xishuangbanna Tropical Botanical Garden in Menglun, Mengla, Yunnan, China.

Plot	*n* Root systems	RDMC (mg g^{-1})	Forks	RTD (g cm^{-3})	SRTA (tips g^{-1})	Root Ca (%)	Root N (%)	Root Mn (mg kg^{-1})
Primary rainforest (RF)	186	310.5 ± 4.3^{b}	272 ± 33^{a}	0.367 ± 0.009^{b}	2186 ± 175^{a}	0.70 ± 0.05^{b}	0.99 ± 0.07^{a}	164.03 ± 13.93^{a}
Secondary evergreen (SE)	138	307.2 ± 4.9^{b}	502 ± 38^{b}	0.362 ± 0.011^{a}	3016 ± 204^{a}	0.22 ± 0.06^{a}	1.13 ± 0.08^{a}	140.29 ± 16.79^{a}
Secondary near rubber plantation (SR)	126	285.6 ± 5.2^{a}	293 ± 40^{a,b}	0.397 ± 0.012^{b}	1659 ± 215^{b}	0.35 ± 0.06^{a}	1.14 ± 0.08^{a}	174.72 ± 16.14^{a}
F-statistic		$F_{(2,447)} = 8.11$	$F_{(2,447)} = 11.70$	$F_{(2,447)} = 2.69$	$F_{(2,447)} = 10.88$	$F_{(2,147)} = 18.93$	$F_{(2,147)} = 1.37$	$F_{(2,147)} = 1.14$
P		***	***	0.07‡	***	***	ns	ns

ANOVA statistics given with associated *P*-values. Letters denote *post hoc* Tukey HSD test groupings. *P*-values are denoted as follows: ns, nonsignificant $P > 0.1$; ‡, marginally significant $P < 0.1$; *, $P < 0.05$; **, $P < 0.01$; ***, $P < 0.001$. RDMC, root dry matter content; RTD, root tissue density; STRA, specific root tip abundance; Ca, calcium, N, nitrogen, Mn, manganese.

angles within the root tissue chemistry ordination space, with root N and Ca roughly being opposed to each other and root Mn arranged orthogonally (Fig. S3B). Root Ca contributed substantially to PCA axis 2 and root N contributed substantially to PCA axis 3 (Table S4).

Root-associated fungal richness, evenness, and diversity

We detected 5771 fungal OTUs from 102 families on the roots of 150 trees from the three sites. The five most speciose fungal families were Glomeraceae (230 OTUs), Herpotrichiellaceae (104 OTUs), Mortierellaceae (89 OTUs), Clavariaceae (52 OTUs), and Agaricaceae (44 OTUs). One-third (34) of the families included in RAF communities contained five or more OTUs. Shannon's diversity of RAF was different among sites ($F_{(2,147)} = 3.089$, $P < 0.05$) and was greater in RF than SE, with SR being statistically indistinguishable from both RF and SE (Fig. 2). Fungal species richness was greater in the two secondary forests than in the primary RF site ($F_{(2,147)} = 6.028$, $P < 0.01$), but species evenness showed the opposite trend ($F_{(2,147)} = 13.440$, $P < 0.05$, Fig. 2).

Relationships of fungal richness, diversity, and evenness to the root and soil environment

Shannon's diversity of RAF increased with total and available soil P, decreased with RDMC, SRTA, the number of root system forks, and RTD, and was unrelated to root tissue N, Ca, or Mn (Fig. S4; Table S5). Fungal species richness decreased with soil total and available soil P, RDMC, SRTA, the number of root system forks, RTD, and root Ca (Fig. S5; Table S5). Fungal assemblage evenness showed the strongest linear relationships of the three diversity measures with any forward-selected variables. Evenness increased with total and available soil P and decreased with the number of root system forks and RTD, but it was unrelated to the remaining five variables (RDMC, SRTA, and root N, Ca, or Mn; Fig. S6; Table S5).

The soil and root environment and root-associated fungal composition

The db-RDA was statistically significant ($F_{(9,140)} = 4.59$, $P < 0.001$), and the constrained ordination axes explained 23% of the variation in root fungal community composition ($I_{total} = 61.91$, $I_{constrained} = 14.12$, $I_{unconstrained} = 47.79$; Fig. 3a). The first four constrained ordination axes were statistically significant (axis 1: $F_{(1,140)} = 19.73$, $P < 0.001$, axis 2: $F_{(1,140)} = 11.52$, $P < 0.001$, axis 3: $F_{(1,140)} = 2.54$, $P < 0.001$, axis 4: $F_{(1,140)} = 1.93$, $P < 0.05$), with the first two axes explaining 75% of the variation explained by the db-RDA (Fig. S7). Composition of tree RAF communities clustered by forest site, illustrating strong site-level differences (Fig. 3a). All terms in the

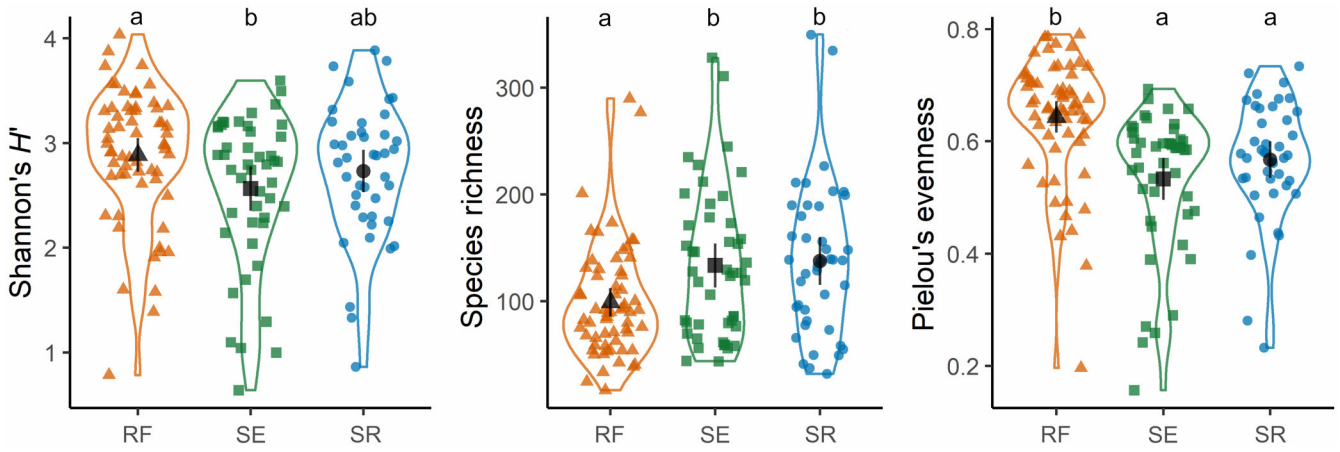

Fig. 2 Diversity (Shannon's *H'*), species richness, and evenness of Fungal ITS2 sequences from fine (1st order) root tips of 150 tropical Angiosperm trees of 66 species from three plots of varying successional status in Xishuangbanna, China. Diversity metrics for root-associated fungal (RAF) communities for each tree are shown as points with outlines showing violin (i.e. mirrored) densities. Black points are means, and bars are 95% confidence intervals. Letters denote statistical grouping from Tukey HSD *post hoc* tests. RF, primary rainforest; SE, secondary evergreen; SR, secondary near rubber plantation.

db-RDA except for root N were either statistically significant or marginally significant (Table S6).

Hierarchical partitioning of environmental variables in the db-RDA revealed that average total and available soil P were the most significant factors constraining fungal community composition (Fig. 3b). Site averages for soil total and available P contributed 76% of the explanatory power of the environment in the db-RDA (Fig. 3b). Of the forward-selected root functional traits and tissue elemental concentrations, root Ca was the strongest predictor, explaining 8% of constrained inertia (i.e. db-RDA R^2), followed by the four root functional traits (RDMC, Forks, RTD, and SRTA), which each explained 3–4% of constrained inertia. Root N and Mn each contributed *c.* 1% to the db-RDA.

Fitted GAM surfaces illustrate environmental relationships to fungal dissimilarities within tree hosts and among sites (Fig. 4). The linear terms of the GAMs were statistically significant for all nine forward-selected variables, and the smooth terms were significant for all variables except for root tissue N and Mn (Table 3). The intercept for the linear term gives the average value for the environmental covariate across fungal assemblages for all three sites. Fitted surfaces for the environmental variables were approximately linear (edf near 1) for SRTA and root tissue N (Fig. 4f,h; Table 3), meaning roughly monotonic increases in these root functional trait measures across the fungal assemblages in the three sites. RTD and Mn concentrations had smooth terms with edf < 1, signifying approximately logarithmic relationships with fungal community dissimilarity among samples in the three sites (Table 3). Accordingly, the fitted surfaces of RTD and root Mn to the constrained ordination space were convex (Fig. 4g,i). The remaining environmental variables (average total soil P, average available soil P, root tissue Ca, the number of root forks, and RDMC) had edf > 1, signifying exponential relationships to fungal community dissimilarity (Table 3). Fitted surfaces of these environmental variables to the compositional variation across the ordination space were roughly concave, with varying complexity (Fig. 4a–e).

Fitted GAMs varied in their goodness of fit to the constrained ordination plane. When fitted as single-variable GAMs, soil total and available P explained > 95% of the variation in fungal compositional differences among sites. Root functional traits each explained between 1% (for RTD) and 14% of the variation (for root forks and RDMC) in fungal assemblages. Root tissue Ca explained 34% of the variation in fungal community dissimilarities, but root N and root Mn each explained ≤ 1% (Table 3). These results were consistent with those from hierarchical variation partitioning (Fig. 4). Fitted GAMs for the entire set of environmental variables (i.e. not only the forward-selected variables) were constructed and plotted (see Tables S6–S8; Figs S8–S10). Soil variables were strongly correlated with db-RDA site scores, each explaining 93–97% of the dissimilarities in fungal composition (Fig. S8; Table S6). Nonforward-selected root functional traits explained 0–25% of the variation in fungal community composition (Fig. S9; Table S8). Similarly, root tissue elemental concentrations other than N, Mn, or Ca each explained 2–21% of the compositional variation (Fig. S10; Table S9).

Discriminating fungal taxa and guilds

FUNGuild was able to classify 57% of OTUs to a fungal guild, revealing differences in the relative abundance of RAF types among sites. The relative abundance of fungal guilds at SR resembled RF more closely than SE (Fig. S11). For example, SE had a much higher relative abundance of ECM fungi and a lower relative abundance of saprophytic fungi than RF or SR (Fig. S11). This pattern was also evident for ECM host trees among sites (Fig. S12). Twenty fungal OTUs contributed ≥ 70% to differences RAF assemblages among sites. SIMPER values ranged from 0.0103 to 0.0439, which represent the relative contribution of each species to overall assemblage dissimilarity (Table 4). These 20 fungal taxa were ordinated on the outskirts of the species space in the db-RDA (Fig. 3a), illustrating their influence on assemblage dissimilarity among the three sites. Seven of these 20 taxa are symbiotrophic ECM fungi, nine are saprotrophic fungi, one (*Diaporthe citrichinensis* F. Huang, K.D. Hyde & HoY. Li) is strictly pathotrophic, another species in the

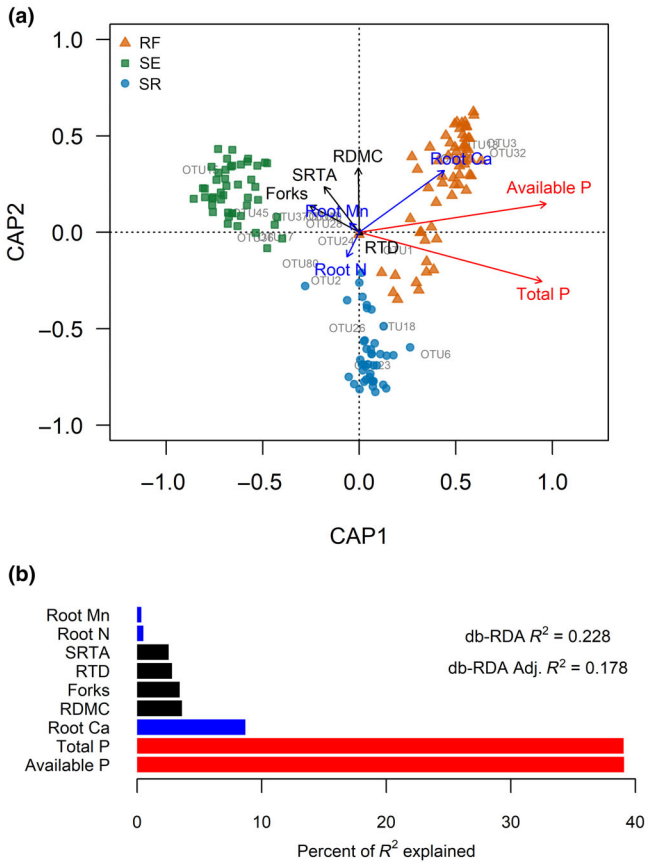

Fig. 3 Analyses of root-associated fungal (RAF) assemblages in relation to the root and soil environment (a) Constrained ordination of fungal ITS2 read counts based on distance-based redundancy analysis (db-RDA) in relation to two soil variables (available and total soil phosphorus, P, shown in red), four root functional traits (number of root forks, root dry matter content (RDMC), root tissue density (RTD), and specific root tip abundance (SRTA), shown in black), and three root tissue elemental concentrations (calcium (Ca), nitrogen (N), and manganese (Mn), shown in blue). Points are individual root systems of 150 trees, colored by collection plot. Species (i.e. operational taxonomic unit (OTU)) scores for the 20 discriminating fungal taxa among sites are plotted in the multivariate space in gray (see Table 4). The scaling of the plot is symmetrical, meaning that both species and site eigenvalues are scaled to their square root. This preserves many of the features of the biplot (i.e. distance interpretation among sites and vector interpretation of environmental variables), without overemphasizing either site or species scores. RF, primary rainforest; SE, secondary evergreen; SR, secondary near rubber plantation. (b) The relative contribution of soil variables, root functional traits, and root chemistry to fungal ITS2 dissimilarity based on hierarchical variation partitioning of variables included in db-RDA. Soil variables are shown in red, root functional traits are colored black, and root tissue elemental concentrations are colored blue.

Tricholomataceae (OTU17) is potentially patho-symbiotrophic, and two are of unknown trophic mode (Table 4). Several of the saprobic taxa might also be present as root endophytes based on their phylogenetic affinities, but this cannot be unequivocally determined. Abundances of OTU17 (Tricholomataceae) differed among all three sites, 16 taxa had OTU read counts which statistically differed among two pairs of sites, and three taxa differed among one pair of sites (Table 4; Fig. S13).

To visualize these compositional trade-offs in fungal guild with environment, we reapplied the db-RDA, grouping fungal taxa by guild. Results confirmed the trends of the SIMPER analysis. The db-RDA by fungal guild showed saprotrophic, and to a lesser-degree AM and pathogenic fungi, to be related to higher levels of soil total P, soil available P, and root Ca (Fig. 5a). Symbiotrophic ECM fungi were positively related to RDMC, RTD, SRTA, and root forks (Fig. 5a). Soil variables were still the most important; however, available P (40%) was a stronger predictor than soil total P (39% vs 23% db-RDA R^2, Fig. 5b). Of the forward-selected root functional traits and tissue elemental concentrations, RDMC was the strongest predictor, explaining 11% of constrained inertia, followed by the root Ca, which each explained 9% of constrained inertia (Fig. 5b).

Discussion

Multivariate community analyses applied to RAF communities of 150 host trees sampled across contrasting tropical forest habitats showed that the soil environment strongly shapes tree RAF communities in this tropical forest, overwhelming functional differences among root systems. This result aligns with previous studies in tropical forests (Essene *et al.*, 2017; Segnitz *et al.*, 2020; Weemstra *et al.*, 2020; Adamo *et al.*, 2021), which also found the soil environment to be the main determinant of mycorrhizal communities, especially for ECM taxa. At least for tree roots in Asian Fagaceae–Lauraceae seasonal tropical forests, a secondary more stochastic environmental filter at the root system level exists (Yan *et al.*, 2022), which selects fungal assemblages according to root morphological and tissue chemistry differences (Jumpponen & Egerton-Warburton, 2005; Beck *et al.*, 2015). We first discuss the role of soils play in shaping plant RAF assemblages, and then we consider the effects of root morphological traits and tissue chemistry on RAF communities.

The soil environment strongly influences plant root–fungi interactions in tropical forests

The principal motivation of this study was to determine the relative strength of the soil environment vs the root system habitat in determining RAF communities. Clear differences in RAF assemblages existed across sites (Fig. 3a), with average total and available soil P accounting for three-quarters of the compositional dissimilarity among root systems; the four root traits and three tissue elemental concentrations explained the remaining quarter (Fig. 3b). Thus, as hypothesized, soil nutrient content is a strong first-order modulator of RAF community composition in tropical forests (Essene *et al.*, 2017; Weemstra *et al.*, 2020; Reichert *et al.*, 2022). Moreover, for GAM fitted surfaces, individual soil variables explained three to four times the variance explained by root traits or tissue elemental concentrations (Fig. 4; Table 3; Fig. S8 vs Figs S9, S10; Table S6 vs Tables S8, S9). Thus, the soil environment most heavily influences tropical tree RAF communities.

Phosphorus is the main limiting nutrient in most lowland tropical forests (Walker & Syers, 1976; Vitousek & Sanford Jr, 1986; Turner *et al.*, 2007; Reed *et al.*, 2011). Soil P drives a trade-off in the acquisition of soil nutrients per the 'do-it-

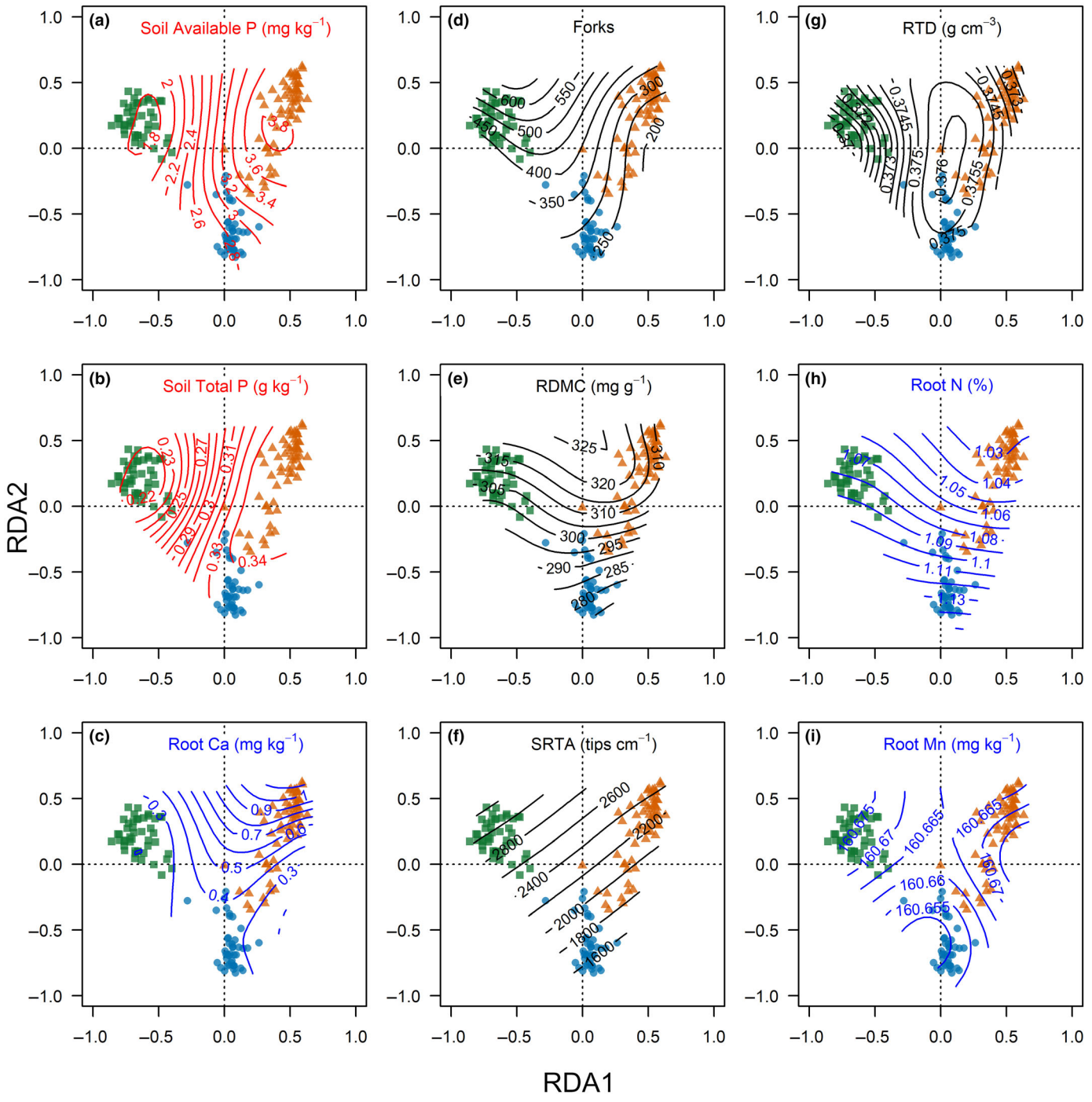

Fig. 4 Constrained ordination (distance-based redundancy analysis (db-RDA)) contour plots of fitted generalized additive model (GAM) surfaces for forward-selected predictor variables (a, soil available phosphorus (P); b, soil total phosphorus; c, root tissue calcium (Ca) concentration; d, number of root system forks; e, root dry matter content (RDMC); f, specific root tip abundance (SRTA); g, root tissue density (RTD); h, root tissue nitrogen (N) concentration; i, root system manganese (Mn) concentration). Points in the ordination space are the db-RDA site (i.e. root-associated fungal (RAF) community) scores, as appearing in Fig. 3(a). Fitted GAM surfaces are overlaid as contour plots in the units of each variable, illustrating how they correspond to RAF composition in the constrained ordination space. Point symbols match the db-RDA in Fig. 3(a).

yourself' vs 'fungal-outsourcing' trade-off (Bergmann *et al.*, 2020; Lugli *et al.*, 2020; Cabugao *et al.*, 2021, Reichert *et al.*, 2022), which has consequences for expressed root morphologies (Hogan *et al.*, 2020). In this study, roots in the site with the highest soil P had fewer root forks, lower root tissue N, and more root tissue Ca than roots from the other two sites (Table 1; Fig. 4). Fewer root forks and lower tissue elemental concentrations typify a 'do it yourself' root functional strategy, where roots forage for and acquire nutrients largely without fungal symbioses (Bergmann *et al.*, 2020). The 'do it yourself' strategy is facultatively AM-associated (McCormack & Iversen, 2019), and we found that saprotrophic fungi were associated with

Table 3 Generalized additive model (GAM) summaries for forward-selected variables.

		Linear term			Smooth term				
Variable	*n*	Int	*t*	*P*	edf	$F_{(edf,9)}$	*P*	Deviance explained (%)	R^2_{adj}
Soil total P (g kg^{-1})	150	0.30	668.1	***	8.89	1673.0	***	99.1	0.99
Soil available P (mg kg^{-1})	150	2.90	294.9	***	8.80	746.8	***	98.0	0.98
Root Ca (%)	150	0.46	14.6	***	5.73	7.6	***	34.2	0.32
Forks	150	347.70	11.6	***	4.40	2.1	***	13.9	0.11
RDMC (mg g^{-1})	150	302.26	86.7	***	4.02	2.2	***	13.9	0.12
SRTA (tips g^{-1})	150	2289.60	14.3	***	1.89	1.3	**	8.5	0.07
RTD (g cm^{-3})	150	0.37	43.2	***	0.48	0.1	ns	0.7	0.16
Root N (%)	150	1.08	25.3	***	0.71	0.1	ns	1.1	0.01
Root Mn (‰)	150	160.7	18.0	***	0.24	<0.1	ns	0.3	<0.01

For each forward-selected variable, a GAM was fit (containing a linear and smooth term) to the two-dimensional constrained ordination (distance-based redundancy analysis (db-RDA)) plane. The smooth term of the model was fit using penalized regression splines. For smooth terms, edf stands for effective degrees of freedom, which controls the flexibility of the term. *P*-values are denoted as follows: ns, nonsignificant $P > 0.1$; *, $P < 0.05$; **, $P < 0.01$; ***, $P < 0.001$. The percent of model deviance explained and adjusted coefficients of determination R^2_{adj} values are given for each GAM. RDMC, root dry matter content; RTD, root tissue density; STRA, specific root tip abundance; Ca, calcium; N, nitrogen; Mn, manganese; P, phosphorus.

these roots (Fig. 5). Additionally, the relationships of soil P to fungal community composition were nonlinear (Kong *et al.*, 2019; Figs 4, S8), reflecting a higher prevalence of AM host trees and suggesting unequal β-diversity turnover of fungal species within RAF communities by site (Figs S5, S6).

After accounting for variation in the soil environment among sites, sites still had very distinct RAF assemblages. Local site differences have also been the most important factor affecting soil fungal community composition in other tropical forest studies (Essene *et al.*, 2017; Weemstra *et al.*, 2020). A greater relative abundance of ECM trees (e.g. Fagaceae and Juglandaceae) relative to AM trees (e.g. Lauraceae and other families) in SE likely led to a higher proportion of ECM fungi (e.g. *Lactarius laccarioides* Wisitr. & Verbeken; Table 4). Trees sampled in the RF site were more associated with saprotrophic fungi (e.g. *Linnemannia amoeboidea* (Gams) Vandepol & Bonito, *Dactylonectria anthuriicola* (A. Cabral & Crous) L. Lombard & Crous). Lastly, trees in the SR site were more associated with pathogens and saprotrophs (i.e. had a higher prevalence of yeast-type and other saprotrophic fungi, such as *Saitozyma podzolica* (Babeva & Reshetova) X.Z. Liu, F.Y. Bai, Groenewald & Boekhout, *Diaporthe citrichinensis*, *Mortierella kuhlmanii* W. Gams, and *Gliocladiopsis* sp.). Other studies have confirmed the high prevalence of saprotrophs in the soils of secondary tropical forests dominated by pioneer and early successional tree species with fast life-history strategies, especially following forest agricultural land use (Liu *et al.*, 2019; Ma *et al.*, 2019; Lan *et al.*, 2022). Our findings show this to be the case for root-inhabiting fungal communities as well. Moreover, root-inhabiting saprotrophic fungi typically decrease when ECM fungi are present since there is direct competition for N between these two fungal guilds (Averill *et al.*, 2014). Land-use legacy effects on fungal communities can result from changes in the soil environment (i.e. pH, as well as the form and availability of nutrients), which are mediated by alterations to the tree community via plant–soil feedbacks (Bahram *et al.*, 2020; Adamo *et al.*, 2021; Lan *et al.*, 2022). Although we cannot explicitly determine the mechanism underlying site differences in RAF communities, our analyses indicate that these differences are not solely because of soil environmental or root functional trait variation but also likely related to dispersal limitation, metacommunity dynamics, and selection of RAF by tree roots or other ecological processes.

In the case of the Xishuangbanna region, rubber (*Hevea brasiliensis* (Willd. ex A. Juss.) Müll. Arg.) cultivation can alter soil fungal assemblages, decreasing the fungal community β-diversity and the relative abundance of Basidiomycota and ECM fungi, without changing soil fungal richness (Ma *et al.*, 2019; Song *et al.*, 2019). Although none of the sites in our study were ever rubber plantations, rubber cultivation is so widespread in the region that it creates a larger matrix of rubber plantations in which natural forest patches inhabit; thus, the effects of rubber plantation land-use are likely strong ecological drivers in the region, potentially even affecting fungal population dynamics in natural forests (Song *et al.*, 2019). Our results largely confirm this finding, wherein we found that ECM fungi dominated the roots of ECM host trees in the SE site where they were most prevalent, but not as much in the RF or SR sites where ECM trees were less common (Figs S12, S13). Therefore, because ECM trees host unique RAF assemblages (Corrales *et al.*, 2018), such changes to soil fungal species pools may occur primarily through the removal of ECM host trees (i.e. fungal species source habitats) and secondarily through the subsequent effects on soil biogeochemical properties (e.g. altered litterfall composition and differing plant–soil feedbacks; Janos, 1980; Alexander & Lee, 2005; Johnson, 2010).

Additionally, ECM host plants, which putatively have more temperate evolutionary origins (Tedersoo *et al.*, 2012; but see Tedersoo & Smith, 2013; Lu & Hedin, 2019), appear to have distinct litterfall and nutrient (i.e. higher C : N ratio) contributions to the soil environment in mixed subtropical and tropical forests (Liang *et al.*, 2020; Segnitz *et al.*, 2020), likely creating plant–soil feedbacks which affect RAF composition (Averill *et al.*, 2022). In tropical and subtropical forests, ECM fungi likely have greater host specificity than AM fungal taxa

Table 4 Similarity percentages and FUNGuild classifications for fungal operational taxonomic units (OTUs) which statistically contributed to Sørensen dissimilarities among root-inhabiting fungal communities within three forest plots in Xishuangbanna.

			Comparison			
OTU	Species	Fungal family	SR–SE	SE–RF	SR–RF	FUNGuild classification and notes
OTU1	*Cladosporium cladosporioides* (Fresen.) G.A. de Vries	Cladosproiaceae	0.0405**	0.0176*	–	Saprotrophic mold commonly found on plant tissues; cosmopolitan in distribution[1]
OTU2	*Saitozyma podzolica* (Babeva & Reshetova) X.Z. Liu, F.Y. Bai, Groenewald & Boekhout	Trimorphomycetaceae	–	0.0237***	0.0247***	Saprotrophic microfungus, anamorphic yeast[2]
OTU3	*Linnemannia camargensis* (Gams) Vandepol & Bonito	Mortierellaceae	–	0.0313***	0.0311***	Saprotrophic soil microfungus[3]
OTU6	*Phialocephala fluminis* Shaerer, J.L. Crane & M.A. Mill	Vibrisseaceae	0.0405***	–	0.0370***	Dark septate symbiotrophic endophyte[4]
OTU7	*Dactylonectria anthuriicola* (A. Cabral & Crous) L. Lombard & Crous	Nectriaceae	–	0.0119***	0.0119***	Saprotrophic microfungus[2]
OTU8	*Lactarius laccarioides* Wisitr. & Verbeken	Russulaceae	0.0439**	0.0424***	–	Symbiotrophic ectomycorrhizal fungus[5]
OTU10	*Lactarius rubrobrunneus* H.T. Le & Nuytinck	Russulaceae	0.0277**	0.0266***	–	Symbiotrophic ectomycorrhizal fungus[5]
OTU13	*Linnemannia amoeboidea* (Gams) Vandepol & Bonito	Mortierellaceae	–	0.0165***	0.0163***	Leaf litter and soil saprotroph[3]
OTU15	*Glutinomyces vulgaris* Nor. Nakam	Hyaloscyphaceae	0.0190***	0.0183***	–	Saprotroph on wood or herbaceous plant tissues[3]
OTU17	Unknown	Tricholomataceae	0.0381*	0.0233***	0.0175***	Possibly symbiotrophic ectomycorrhizal fungus[3,6]
OTU18	*Diaporthe citrichinensis* F. Huang, K.D. Hyde & Hong Y. Li	Valsaceae	–	–	0.0108***	Melanose endophytic pathogenic microfungus[7]
OTU23	*Helotiales* sp.	Hyaloscyphaceae	0.0164***	–	0.0136***	Saprotroph on woody and herbaceous plant tissue[3]
OTU24	*Tomentella* sp.	Thelephoraceae	–	–	0.0189***	Symbiotrophic ectomycorrhizal clavaroid corticioid fungi[3]
OTU26	Unknown	Class: Sordariomycetes	0.0197***	–	0.0196***	Unknown
OTU28	*Clavulina* sp.	Clavulinaceae	0.0109***	0.0103***	–	Symbiotrophic ectomycorrhizal fungus[5]
OTU32	*Linnemannia camargensis* (Gams) Vandepol & Bonito	Mortierellaceae	–	0.0311***	0.0313***	Litter and soil saprotroph, may act as a root endophyte[3]
OTU36	*Hydropus* sp.	Tricholomataceae	0.0288***	0.0278***	–	Saprotroph on litter and wood[8]
OTU37	–	Cortinariaceae	0.0252**	0.0225***	–	Symbiotrophic ectomycorrhizal fungus[3]
OTU45	*Oidiodendron maius* G.L. Barron	Myxotrichaceae	0.0156***	0.0130***	–	Biotrophic ericoid dark septate endophyte; has the potential to act as a root parasite in some cases[4]
OTU80	–	Order: Trechisporales	–	–	0.0169**	Unknown

SIMPER statistics are given for each pairwise comparison between plots. False-discovery rate-corrected probabilities for Kruskal–Wallis tests are denoted as follows: ns, nonsignificant $P > 0.1$; *, $P < 0.05$; **, $P < 0.01$; ***, $P < 0.001$. RF, primary rainforest; SE, secondary evergreen; SR, secondary near rubber plantation.

[1]Bensch *et al*. (2010).
[2]Sterkenburg *et al*. (2015).
[3]Cannon & Kirk (2007), Vandepol *et al*. (2020).
[4]Newsham (2011).
[5]Tedersoo *et al*. (2010a).
[6]Designated as ectomycorrhizal (ECM) based on close BLAST matches to other ECM sequences from China including JQ991905, MK770274, and JQ991904.
[7]F. Huang *et al*. (2015).
[8]Tedersoo *et al*. (2014).

(Klironomos, 2000; Smith & Read, 2008; Tedersoo *et al*., 2010b). Yet, because of AM tree dominance in these forests, ECM host–fungal assemblages are context-dependent, being influenced by neighboring ECM trees and reflecting landscape-scale β-diversity patterns in host plants and fungi, which are each sorted by the soil environment (Smith *et al*., 2011; Peay *et al*., 2013; Corrales *et al*., 2018; Averill *et al*., 2019; Weemstra *et al*., 2020; Ferlian *et al*., 2021). However, a similar study to this

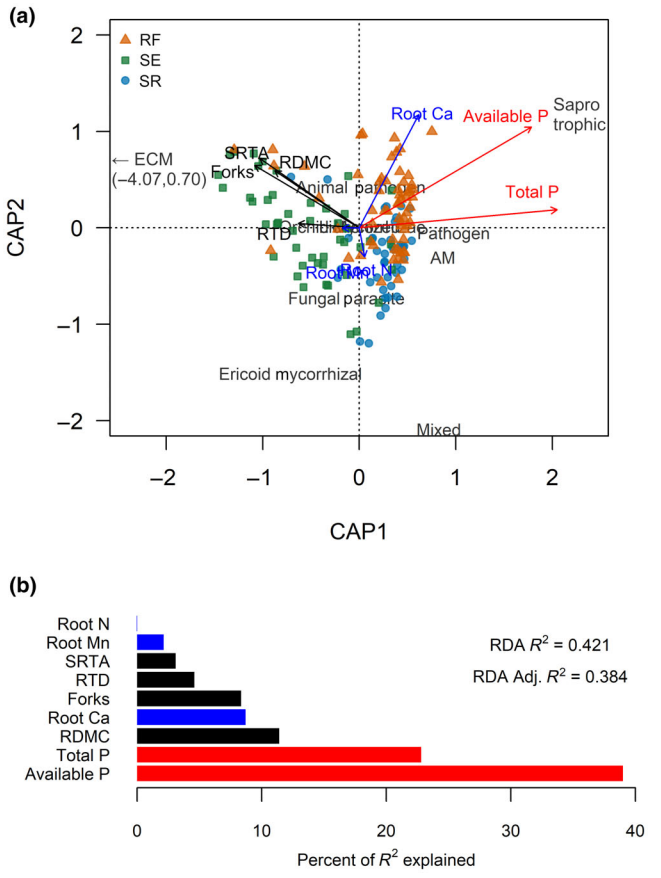

Fig. 5 Analyses of root-associatad FUNGuild composition in relation to the root and soil enviroment. (a) Distance-base redundancy analysis (db-RDA) by FUNGuild fungal guild classification. As in Fig. 3, symmetrical plot scaling is used in this figure. RF, primary rainforest; SE, secondary evergreen; SR, secondary near rubber plantation. This db-RDA is statistically significant ($F_{(9,140)} = 4.27$, $P < 0.001$), and the constrained ordination axes explained 22% of the variation in root fungal community composition ($I_{total} = 15.92$, $I_{constrained} = 5.10$, $I_{unconstrained} = 10.82$). Only the first two constrained ordination axes are statistically significant (axis 1: $F_{(1,140)} = 51.68$, $P < 0.001$; axis 2: $F_{(1,140)} = 7.67$, $P < 0.01$). Additionally, soil available phosphorus (P) ($F_{(1,140)} = 32.63$, $P < 0.001$), soil total P ($F_{(1,140)} = 14.28$, $P < 0.001$), forks ($F_{(1,140)} = 3.29$, $P < 0.05$), root dry matter content (RDMC) ($F_{(1,140)} = 7.90$, $P < 0.001$), specific root tip abundance (STRA) ($F_{(1,140)} = 2.47$, $P = 0.058$), and root tissue density (RTD) ($F_{(1,140)} = 3.07$, $P < 0.05$) are statistically significant terms in this constrained ordination. (b) The relative contribution of soil variables, root functional traits, and root chemistry to fungal guild dissimilarity. Soil variables are shown in red, root functional traits are colored black, and root tissue elemental concentrations are colored blue. N, nitrogen; Mn, manganese; Ca, calcium.

one that sequenced root-inhabiting fungal communities with ECM (primarily Fagaceae) and AM trees in a mixed secondary forest in Japan found nontypical (i.e. novel) assemblages of RAF. They concluded that ECM fungi from Fagaceae trees can colonize nearby AM hosts and thereby influence interactions between AM fungi and their host trees (Toju *et al.*, 2014). Thus, the soil environment acts as a first-order control on RAF communities, environmentally filtering fungi from the available species pool, but the composition of tree hosts can also affect RAF assemblages.

The secondary role of the root system environment in influencing plant root–fungi interactions in tropical forest

After the soil environment, a second environmental filter shaping fungal assemblages occurs at the root system level (Xia *et al.*, 2021; Yan *et al.*, 2022). The four forward-selected root traits typify a trade-off in root construction strategy for tropical trees. On one end of the trade-off are dense, often lignified roots (e.g. Fagaceae). On the other are highly branched roots with many first-order tips per unit length (e.g. 'herringbone' topologies of Lauraceae and Myristicaceae). The fine root tips of Fagaceae trees are almost always colonized by ECM, while Lauraceae roots are associated with AM, usually along the entire absorptive root length. Thus, root topology is a central axis of functional differentiation that shapes RAF assemblages (Alzarhani *et al.*, 2019; Yan *et al.*, 2022). Moreover, root branching is a crucial trait that relates to both aboveground and belowground resource-acquisition strategies (Liese *et al.*, 2017; Bergmann *et al.*, 2020) and can act as a functional filter for RAF composition, especially AM fungi.

The soil environment affects root functional morphology and root tissue chemistry, which both successively shape RAF composition. Root systems in primary RF had less branching than the two secondary forest sites (Table 2). Despite not being able to control perfectly for host identity at the species level, this result supported our hypothesis that roots in primary forests express more conservative functional strategies (Hogan *et al.*, 2020). Although intraspecific trait variation may contribute slightly, we largely attribute differences in root morphologies among sites to interspecific variation (Fig. S14; Table S10). In addition, root tissue Ca was significantly greater in RF relative to the two secondary forest sites, illustrating how variation in tissue chemistry, except root tissue nitrogen, accompanies morphological differences (Hogan *et al.*, 2020, 2021). RAF β-diversity and richness were positively related to root branching (i.e. acquisitiveness), whereas fungal diversity, richness, and evenness all decreased with increasing root branching and tip abundance (i.e. acquisitiveness). This result suggests that fungal identity (i.e. species or assemblage composition) is more important than fungal species richness in shaping RAF community–root system interactions (Ferlian *et al.*, 2021), especially for acquisitive root morphologies. Root–fungi interactions (e.g. nutrient transfer) are in some cases highly species-specific (Smith & Read, 2008), and the presence of other fungal species (e.g. saprotrophic or pathogenic fungi) potentially reduces the benefit of certain species-specific symbioses (Churchland & Grayston, 2014). Therefore, for most AM-associated tropical trees, with acquisitive root strategies (e.g. high SRL, low branchiness, and high tissue Ca concentrations), root strategy likely plays an important role in determining RAF composition.

Root morphology and tissue chemistry selected for RAF community functional guild composition. We observed a positive association between ECM fungi and root system topological complexity (i.e. high SRTA, more root forks) and root tissue density. Additionally, for AM angiosperms, which dominate these forests, root tissue Ca, Mn, and N concentrations are key root

elements that shape fungal assemblages. All three elements have confirmed physiological functions in initiating AM tree-mycorrhizal symbioses (Bonfante & Genre, 2010). Therefore, a clear difference in root functional trait associations to fungal communities emerged among sites, which indicates differentiation along the 'fungal-symbiosis' dimension of root economics (Yan *et al.*, 2022). Trees in RF were most strongly associated with saprotrophic and AM fungi, those in ECM-dominated SE were most strongly associated with ECM fungi, and trees in AM-dominated SR showed a higher prevalence of pathogenic fungi intermixed with saprotrophic and AM fungi, which is consistent with other research (Song *et al.*, 2019; Adamo *et al.*, 2021; Lan *et al.*, 2022).

Among the site-representative samples of tropical tree roots in this study, root tissue calcium and manganese were important for driving RAF community dissimilarity. In Xishuangbanna, AM colonization rates range from 6 to 91%, with significant variation among plant species but not forest types (Muthukumar *et al.*, 2003b). On average, 35% of roots are colonized by AM fungi in both primary and secondary forests, but AM spore densities in secondary forest bulk soil are more than double those in primary forest (Muthukumar *et al.*, 2003b). Thus, AM roots are highly selective to fungal taxa and likely maintain similar rates of colonization in comparable soil environments, despite potential differences in spore abundance, species composition of colonizing AM fungi, or root morphological variability (Johnson, 2010; Lugli *et al.*, 2020). First, calcium increase (termed 'spiking') in root tissues is a chemical hallmark of the molecular signaling pathway in fine root tissues that facilitates symbiotic AM establishment (Kosuta *et al.*, 2008; Bonfante & Genre, 2010; Luginbuehl & Oldroyd, 2016). Calcium spiking occurs within the nucleus of root cortical cells via increased calcium channel activity, altering root gene expression and stimulating AM hyphal penetration and arbuscule development. Second, manganese must be actively taken up by plant roots (with or without mycorrhizal symbiosis) and is central to plant functioning, especially for the light reactions of photosynthesis. Certain AM fungi (e.g. *Glomus* and *Paraglomus* spp.) increase Mn concentrations in root tissues by aiding in Mn uptake (Wu *et al.*, 2011; Bagheri *et al.*, 2012). Therefore, root tissue chemistry, specifically tissue concentrations of cations like Ca and Mn, functionally differentiates roots of AM and ECM host trees and influences RAF assemblages.

Finally, we expected discriminating fungal taxa among sites to jointly reflect variation in soil environmental filters and host tree dominance of AM vs ECM tree species. Analyses by fungal guild showed RF to be associated with AM fungi, which was strongly correlated to root Ca. Lauraceae, Myristicaceae, and other AM trees dominated RF, although there were rare ECM trees intermixed. Indeed, there was mixed support for the presence of AM fungi solely driving site-specific differences, as the analysis by fungal guild also showed ECM fungi to be present in RF. The combined importance of the soil and root system environment in this plot likely reflects variation in AM host assemblage (and to a lesser degree ECM host-fungal assemblage) selection with forest age (Matsuoka *et al.*, 2016; Kuang *et al.*, 2021). Future research might measure the ecosystem effects of such tropical tree host–fungal community interactions, potentially exploring how plant–soil and fungal–soil interactions influence biogeochemical cycles (e.g. Koide *et al.*, 2014; Xia *et al.*, 2021).

Conclusion

Tropical tree root-inhabiting fungal assemblages are shaped by a series of successive environmental filters: the soil and the root environment. Despite sampling a variety of root functional strategies across a range of soil environments in three tropical forest stands in Southwestern China, soil environmental differences were paramount among sites. However, tree roots did function as a second, albeit weaker, environmental filter to select RAF assemblages. For ECM trees, this is primarily a root morphological filter driven by architectural complexity (i.e. the number of tips and forks) and variation in root tissue construction cost and longevity (i.e. RDMC and RTD). For AM angiosperms, which dominate these forests, root tissue Ca and Mn concentrations are key root elements that are most related to variation in fungal assemblages, both of which have confirmed physiological functions in tree-mycorrhizal symbioses. Accordingly, clear differences in the type of functional associations can arise among locally variable tropical forest sites. In our study, trees in primary forest were most strongly associated with either saprotrophic or mycorrhizal fungi. Those in ECM-dominated secondary forests were most strongly associated with biotrophic fungi (including ECM fungi), whereas trees in AM-dominated secondary forests were most strongly associated with pathogenic and saprotrophic fungi.

Acknowledgements

This research was funded by a 2018 Garden Club of America Award in Tropical Botany and a research fellowship from the FIU Tropics program at the Institute of Environment, Florida International University. JAH received financial support from the FIU University Graduate School Dissertation Year Fellowship. The Xishuangbanna Tropical Botanical Garden at the Chinese Academy of Sciences provided additional support (NSFC grant 32061123003). We acknowledge the field and laboratory assistance of Iwan Guan, Run Shen, Yuan Zi, Xiao (Lilly) Taiyang, Dong-Hai Yang, and Wenfu Zhang. Finally, we are grateful to the Smith Laboratory at the University of Florida, Department of Plant Pathology, for providing laboratory resources and training to JAH. We thank several anonymous reviewers for their insightful comments and suggestions.

Competing interests

None declared.

Author contributions

JAH, OJV-B and CB conceived the idea for the study. JAH and CB secured funding. JAH, MAJ, MES and AC planned the sampling strategy of the study. JAH conducted the fieldwork with

the help of XS, Y-HH, JY and MC. JY, XS and MC provided financial support for fieldwork. MES facilitated and oversaw laboratory work, which was done by JAH with the guidance and supervision of MAJ. MAJ prepared samples for sequencing and completed bioinformatics. Analyses and manuscript preparation were done by JAH. All co-authors provided comments on manuscript drafts and final approval for manuscript submission.

ORCID

Christopher Baraloto https://orcid.org/0000-0001-7322-8581
Min Cao https://orcid.org/0000-0002-4497-5841
Adriana Corrales https://orcid.org/0000-0001-9885-4634
J. Aaron Hogan https://orcid.org/0000-0001-9806-3074
Yue-hua Hu https://orcid.org/0000-0003-3027-1410
Michelle A. Jusino https://orcid.org/0000-0002-3284-4254
Matthew E. Smith https://orcid.org/0000-0002-0878-0932
Xiaoyang Song https://orcid.org/0000-0001-9529-1418
Oscar J. Valverde-Barrantes https://orcid.org/0000-0002-7327-7647
Jie Yang https://orcid.org/0000-0002-4444-8240

Data availability

All data products, including environmental data, root functional trait data, root tissue elemental concentration data, AMPtk bioinformatics processing code and output from ITS2 sequences and R code used in data analyses for this study, are available at this OSF archive: https://osf.io/hn3by/. Plant rbcL sequences have been uploaded to GenBank. GenBank accession nos. BankIt2510297: OK562430–OK562579. Raw Illumina sequence data are deposited in the Sequence Read Archive (SRA) of the National Center for Biotechnology Information (PRJNA923807).

References

Adamo I, Ortiz-Malavasi E, Chazdon R, Chaverri P, ter Steege H, Geml J. 2021. Soil fungal community composition correlates with site-specific abiotic factors, tree community structure, and forest age in regenerating tropical rainforests. *Biology* **10**: 1120.

Alexander IJ, Lee S. 2005. Mycorrhizas and ecosystem processes in tropical rain forest: implications for diversity. In: Burslem D, Pinard M, Hartley S, eds. *Biotic interactions in the tropics: their role in the maintenance of species diversity*. Cambridge, UK: Cambridge University Press, 165–203.

Alzarhani AK, Clark DR, Underwood GJC, Ford H, Cotton TEA, Dumbrell AJ. 2019. Are drivers of root-associated fungal community structure context-specific? *The ISME Journal* **13**: 1330–1344.

Averill C, Bhatnagar JM, Dietze MC, Pearse WD, Kivlin SN. 2019. Global imprint of mycorrhizal fungi on whole-plant nutrient economics. *Proceedings of the National Academy of Sciences, USA* **116**: 23163–23168.

Averill C, Fortunel C, Maynard DS, van den Hoogen J, Dietze MC, Bhatnagar JM, Crowther TW. 2022. Alternative stable states of the forest microbiome are maintained through positive feedbacks. *Nature Ecology & Evolution* **6**: 375–382.

Averill C, Turner BL, Finzi AC. 2014. Mycorrhiza-mediated competition between plants and decomposers drives soil carbon storage. *Nature* **505**: 543–545.

Bagheri V, Shamshiri M, Shirani H, Roosta H. 2012. Nutrient uptake and distribution in mycorrhizal pistachio seedlings under drought stress. *Journal of Agricultural Science and Technology* **14**: 1591–1604.

Bahram M, Netherway T, Hildebrand F, Pritsch K, Drenkhan R, Loit K, Anslan S, Bork P, Tedersoo L. 2020. Plant nutrient-acquisition strategies drive topsoil microbiome structure and function. *New Phytologist* **227**: 1189–1199.

Baraloto C, Vleminckx J, Engel J, Petronelli P, Dávila N, Ríos M, Valderrama Sandoval EH, Mesones I, Guevara Andino JE, Fortunel C *et al.* 2021. Biogeographic history and habitat specialization shape floristic and phylogenetic composition across Amazonian forests. *Ecological Monographs* **91**: e01473.

Beck S, Powell JR, Drigo B, Cairney JWG, Anderson IC. 2015. The role of stochasticity differs in the assembly of soil- and root-associated fungal communities. *Soil Biology and Biochemistry* **80**: 18–25.

Benjamini Y, Hochberg Y. 1995. Controlling the false discovery rate: a practical and powerful approach to multiple testing. *Journal of the Royal Statistical Society Series B (Methodological)* **57**: 289–300.

Bensch K, Groenewald JZ, Dijksterhuis J, Starink-Willemse M, Andersen B, Summerell BA, Shin HD, Dugan FM, Schroers HJ, Braun U *et al.* 2010. Species and ecological diversity within the *Cladosporium cladosporioides* complex (Davidiellaceae, Capnodiales). *Studies in Mycology* **67**: 1–94.

Bergmann J, Weigelt A, van der Plas F, Laughlin DC, Kuyper TW, Guerrero-Ramirez N, Valverde-Barrantes OJ, Bruelheide H, Freschet GT, Iversen CM *et al.* 2020. The fungal collaboration gradient dominates the root economics space in plants. *Science Advances* **6**: eaba3756.

Blanchet FG, Legendre P, Borcard D. 2008. Forward selection of explanatory variables. *Ecology* **89**: 2623–2632.

Bonfante P, Genre A. 2010. Mechanisms underlying beneficial plant–fungus interactions in mycorrhizal symbiosis. *Nature Communications* **1**: 48.

Brazee NJ, Lindner DL. 2013. Unravelling the *Phellinus pini* s.l. complex in North America: a multilocus phylogeny and differentiation analysis of *Porodaedalea*. *Forest Pathology* **43**: 132–143.

Brundrett MC. 2002. Coevolution of roots and mycorrhizas of land plants. *New Phytologist* **154**: 275–304.

Cabugao KG, Yaffar D, Stenson N, Childs J, Phillips J, Mayes MA, Yang X, Weston DJ, Norby RJ. 2021. Bringing function to structure: root–soil interactions shaping phosphatase activity throughout a soil profile in Puerto Rico. *Ecology and Evolution* **11**: 1150–1164.

Cannon PF, Kirk PM. 2007. *Fungal families of the world*. London, UK: CABI, 456.

Chen W, Koide RT, Adams TS, DeForest JL, Cheng L, Eissenstat DM. 2016. Root morphology and mycorrhizal symbioses together shape nutrient foraging strategies of temperate trees. *Proceedings of the National Academy of Sciences, USA* **113**: 8741–8746.

Churchland C, Grayston SJ. 2014. Specificity of plant–microbe interactions in the tree mycorrhizosphere biome and consequences for forest C cycling. *Frontiers in Microbiology* **5**: 261.

Clarke KR. 1993. Non-parametric multivariate analyses of changes in community structure. *Australian Journal of Ecology* **18**: 117–143.

Corrales A, Henkel TW, Smith ME. 2018. Ectomycorrhizal associations in the tropics – biogeography, diversity patterns and ecosystem roles. *New Phytologist* **220**: 1076–1091.

Essene AL, Shek KL, Lewis JD, Peay KG, McGuire KL. 2017. Soil type has a stronger role than dipterocarp host species in shaping the ectomycorrhizal fungal community in a Bornean lowland tropical rain forest. *Frontiers in Plant Science* **8**: 1828.

Fei S, Kivlin SN, Domke GM, Jo I, LaRue EA, Phillips RP. 2022. Coupling of plant and mycorrhizal fungal diversity: its occurrence, relevance and possible implicaitons under global change. *New Phytologist* **234**: 1960–1966.

Ferlian O, Goldmann K, Eisenhauer N, Tarkka MT, Buscot F, Heintz-Buschart A. 2021. Distinct effects of host and neighbour tree identity on arbuscular and ectomycorrhizal fungi along a tree diversity gradient. *IMSE Communications* **1**: 40.

Fine PVA, Kembel SW. 2011. Phylogenetic community structure and phylogenetic turnover across space and edaphic gradients in western Amazonian tree communities. *Ecography* **34**: 552–565.

Gourmelon V, Maggia L, Powell JR, Gigante S, Hortal S, Gueunier C, Letellier K, Carriconde F. 2016. Environmental and geographical factors structure soil

microbial diversity in New Caledonian ultramafic substrates: a metagenomic approach. *PLoS ONE* **11**: e0167405.

van der Heijden MGA, Martin FM, Selosse M-A, Sanders IR. 2015. Mycorrhizal ecology and evolution: the past, the present, and the future. *New Phytologist* **205**: 1406–1423.

Hetrick BAD. 1991. Mycorrhizas and root architecture. *Experientia* **47**: 355–362.

Hogan JA, Valverde-Barrantes OJ, Ding Q, Xu H, Baraloto C. 2020. Morphological variation of fine root systems and leaves in primary and secondary tropical forests of Hainan Island, China. *Annals of Forest Science* **77**: 79.

Hogan JA, Valverde-Barrantes OJ, Tang W, Ding Q, Xu H, Baraloto C. 2021. Evidence of elemental homeostasis in fine root and leaf tissues of saplings across a fertility gradient in tropical montane forest in Hainan, China. *Plant and Soil* **460**: 625–646.

Huang F, Udayanga D, Wang X, Hou X, Mei X, Fu Y, Hyde KD, Li H. 2015. Endophytic Diaporthe associated with Citrus: a phylogenetic reassessment with seven new species from China. *Fungal Biology* **119**: 331–347.

Huang XC, Ci XQ, Conran JG, Li J. 2015. Application of DNA barcodes in Asian tropical trees – a case study from Xishuangbanna Nature Reserve, southwest China. *PLoS ONE* **10**: e0129295.

Ihrmark K, Bödeker I, Cruz-Martinez K, Friberg H, Kubartova A, Schenck J, Strid Y, Stenlid J, Brandström-Durling M, Clemmensen KE. 2012. New primers to amplify the fungal ITS2 region – evaluation by 454-sequencing of artificial and natural communities. *FEMS Microbiology Ecology* **82**: 666–677.

Janos DP. 1980. Mycorrhizae influence tropical succession. *Biotropica* **12**: 56–64.

Johnson NC. 2010. Resource stoichiometry elucidates the structure and function of arbuscular mycorrhizas across scales. *New Phytologist* **185**: 631–647.

Jumpponen A, Egerton-Warburton LM. 2005. Mycorrhizal fungi in successional environments: a community assembly model incorporating host plant, environmental, and biotic filters. In: Dighton J, White JF, Oudemans P, eds. *The fungal community: its organization and role in the ecosystem, 3rd edn.* Boca Raton, FL, USA: Taylor & Francis Group, CRC Press, 139–168.

Kenrick P, Strullu-Derrien C. 2014. The origin and early evolution of roots. *Plant Physiology* **166**: 570–580.

Klironomos JN. 2000. Host-specificity and functional diversity among arbuscular mycorrhizal fungi. In: Bell CR, Brylinski M, Johnson-Green P, eds. *Microbial biosystems: new frontiers. Proceedings of the 8th International Symposium on microbial ecology.* Halifax, NS, Canada: Atlantic Canada Society from Microbial Ecology, 845–851.

Kohout P, Sudová R, Janoušková M, Čtvrtlíková M, Hejda M, Pánková H, Slavíková R, Štajerová K, Vosátka M, Sýkorová Z. 2014. Comparison of commonly used primer sets for evaluating arbuscular mycorrhizal fungal communities: is there a universal solution? *Soil Biology and Biochemistry* **68**: 482–493.

Koide RT, Fernandez C, Malcolm G. 2014. Determining place and process: functional traits of ectomycorrhizal fungi that affect both community structure and ecosystem function. *New Phytologist* **201**: 433–439.

Kong D, Wang J, Wu H, Valverde-Barrantes OJ, Wang R, Zeng H, Kardol P, Zhang H, Feng Y. 2019. Nonlinearity of root trait relationships and the root economics spectrum. *Nature Communications* **10**: 2203.

Kosuta S, Hazledine S, Sun J, Miwa H, Morris RJ, Downie JA, Oldroyd GE. 2008. Differential and chaotic calcium signatures in the symbiosis signaling pathway of legumes. *Proceedings of the National Academy of Sciences, USA* **105**: 9823–9828.

Kress WJ, Erickson DL. 2007. A two-locus global DNA barcode for land plants: the coding rbcL gene complements the non-coding trnH-psbA spacer region. *PLoS ONE* **2**: e508.

Kuang J, Han S, Chen Y, Bates CT, Wang P, Shu W. 2021. Root-associated fungal community reflects host spatial co-occurrence patterns in a subtropical forest. *ISME Communications* **1**: 65.

Lai J, Zou Y, Zhang J, Peres-Neto P. 2021. Generalizing hierarchical and variation partitioning in multiple regression and canonical analyses using the RDACCA.HP R package. *Methods in Ecology & Evolution* **13**: 782–788.

Lan G, Yang C, Wu Z, Sun R, Chen X, Zhang X. 2022. Network complexity of rubber plantations is lower than tropical forests for soil bacteria but not for fungi. *Soil* **8**: 149–161.

Legendre P, Anderson MJ. 1999. Distance-based redundancy analysis: testing multispecies responses in multifactorial ecological experiments. *Ecological Monographs* **69**: 1–24.

Legendre P, Legendre L. 2012. *Numerical ecology.* Oxford, UK: Elsevier.

Leibold MA, Chase JM. 2018. *Metacommunity ecology, vol. 59.* Princeton, NJ, USA: Princeton University Press.

Leibold MA, Holyoak M, Mouquet N, Amarasekare P, Chase JM, Hoopes MF, Holt RD, Shurin JB, Law R, Tilman D *et al.* 2004. The metacommunity concept: a framework for multi-scale community ecology. *Ecology Letters* **7**: 601–613.

Lekberg Y, Vasar M, Bullington LS, Sepp SK, Antunes PM, Bunn R, Larkin BG, Öpik M. 2018. More bang for the buck? Can arbuscular mycorrhizal fungal communities be characterized adequately alongside other fungi using general fungal primers? *New Phytologist* **220**: 971–976.

Liang M, Johnson D, Burslem DFRP, Yu S, Fang M, Taylor JD, Taylor AFS, Helgason T, Liu X. 2020. Soil fungal networks maintain local dominance of ectomycorrhizal trees. *Nature Communications* **11**: 2636.

Liese R, Alings K, Meier IC. 2017. Root branching is a leading root trait of the plant economics spectrum in temperate trees. *Frontiers in Plant Science* **8**: 315.

Lindner DL, Banik MT. 2009. Effects of cloning and root-tip size on observations of fungal ITS sequences from *Picea glauca* roots. *Mycologia* **101**: 157–165.

Liu C, Xiang W, Zou L, Lei P, Zeng Y, Shuai O, Deng X, Fang X, Liu Z, Peng C. 2019. Variation in the functional traits of fine roots is linked to phylogenetics in the common tree species of Chinese subtropical forests. *Plant and Soil* **436**: 1–18.

Lovelock CE, Ewel JJ. 2005. Links between tree species, symbiotic fungal diversity and ecosystem functioning in simplified tropical ecosystems. *New Phytologist* **167**: 219–228.

Lu M, Hedin L. 2019. Global plant–symbiont organization and emergence of biogeochemical cycles resolved by evolution-based trait modeling. *Nature Ecology & Evolution* **3**: 239–250.

Luginbuehl L, Oldroyd GE. 2016. Calcium signaling and transcriptional regulation in arbuscular mycorrhizal symbiosis. In: Martin FM, ed. *Molecular mycorrhizal symbiosis.* Hoboken, NJ, USA: John Wiley & Sons, 125–140.

Lugli LF, Andersen KM, Aragão LE, Cordeiro AL, Cunha HF, Fuchslueger L, Meir P, Mercado LM, Oblitas E, Quesada CA. 2020. Multiple phosphorus acquisition strategies adopted by fine roots in low-fertility soils in Central Amazonia. *Plant and Soil* **450**: 49–63.

Ma H, Zou W, Yang J, Hogan JA, Xu H, Chen J. 2019. Dominant tree species shape soil microbial community via regulating assembly processes in planted subtropical forests. *Forests* **10**: 978.

Ma Z, Guo D, Xu X, Lu M, Bardgett RD, Eissenstat DM, McCormack ML, Hedin LO. 2018. Evolutionary history resolves global organization of root functional traits. *Nature* **555**: 94–97.

Maciá-Vicente JG, Nam B, Thines M. 2020. Root filtering, rather than host identity or age, determines the composition of root-associated fungi and oomycetes in three naturally co-occurring Brassicaceae. *Soil Biology and Biochemistry* **146**: 107806.

Matsuoka S, Mori AS, Kawaguchi E, Hobara S, Osono T. 2016. Disentangling the relative importance of host tree community, abiotic environment and spatial factors on ectomycorrhizal fungal assemblages along an elevation gradient. *FEMS Microbiology Ecology* **92**: fiw044.

McCormack ML, Dickie IA, Eissenstat DM, Fahey TJ, Fernandez CW, Guo D, Helmisaari HS, Hobbie EA, Iversen CM, Jackson RB. 2015. Redefining fine roots improves understanding of below-ground contributions to terrestrial biosphere processes. *New Phytologist* **207**: 505–518.

McCormack ML, Iversen CM. 2019. Physical and functional constraints on viable belowground acquisition strategies. *Frontiers in Plant Science* **10**: 1215.

Muthukumar T, Sha L, Yang X, Cao M, Tang J, Zheng Z. 2003a. Distribution of roots and arbuscular mycorrhizal associations in tropical forest types of Xishuangbanna, southwest China. *Applied Soil Ecology* **22**: 241–253.

Muthukumar T, Sha L, Yang X, Cao M, Tang J, Zheng Z. 2003b. Mycorrhiza of plants in different vegetation types in tropical ecosystems of Xishuangbanna, southwest China. *Mycorrhiza* **13**: 289–297.

Newsham KK. 2011. A meta-analysis of plant responses to dark septate root endophytes. *New Phytologist* **190**: 783–793.

Nguyen NH, Song Z, Bates ST, Branco S, Tedersoo L, Menke J, Schilling JS, Kennedy PG. 2016. FUNGuild: an open annotation tool for parsing fungal community datasets by ecological guild. *Fungal Ecology* **20**: 241–248.

Nilsson RH, Larsson K-H, Taylor AFS, Bengtsson-Palme J, Jeppesen TS, Schigel D, Kennedy P, Picard K, Glöckner FO, Tedersoo L *et al.* 2018. The UNITE database for molecular identification of fungi: handling dark taxa and parallel taxonomic classifications. *Nucleic Acids Research* **47**(D1): D259–D264.

Oksanen J, Blanchet F, Friendly M, Kindt R, Legendre P, McGlinn D, Minchin PR, O'Hara RB, Simpson GL, Stevens HH *et al.* 2020. *vegan: community ecology package*. R package v.2.5-7. [WWW document] URL https://cran.r-project.org/package=vegan [accessed 1 January 2022].

Palmer JM, Jusino MA, Banik MT, Lindner DL. 2018. Non-biological synthetic spike-in controls and the AMPtk software pipeline improve mycobiome data. *PeerJ* **6**: e4925.

Pan XZ, Guo ZY, Pan K. 2019. *Protocols for stand soil observation and measurement in terrestrial ecosystems*. Beijing, China: China Environmental Publishing House.

Peay KG, Baraloto C, Fine PVA. 2013. Strong coupling of plant and fungal community structure across western Amazonian rainforests. *The ISME Journal* **7**: 1852–1861.

Peay KG, Bidartondo MI, Elizabeth AA. 2010a. Not every fungus is everywhere: scaling to the biogeography of fungal–plant interactions across roots, shoots and ecosystems. *New Phytologist* **185**: 878–882.

Peay KG, Garbelotto M, Bruns TD. 2010b. Evidence of dispersal limitation in soil microorganisms: isolation reduces species richness on mycorrhizal tree islands. *Ecology* **91**: 3631–3640.

Peres-Neto PR, Legendre P, Dray S, Borcard D. 2006. Variation partitioning of species data matrices: estimation and comparison of fractions. *Ecology* **87**: 2614–2625.

Pileou EC. 1966. The measurement of diversity in different types of biological collections. *Journal of Theoretical Biology* **13**: 131–144.

Pregitzer KS, DeForest JL, Burton AJ, Allen MF, Ruess RW, Hendrick RL. 2002. Fine root architecture of nine north American trees. *Ecological Monographs* **72**: 293–309.

R Core Team. 2021. *R: a language and environment for statistical computing v.4.0.5*. Vienna, Austria: R Foundation for Statistical Computing. [WWW document] URL https://cran.r-project.org/ [accessed 1 January 2022].

Reed SC, Townsend AR, Taylor PG, Cleveland CC. 2011. Phosphorus cycling in tropical forests growing on highly weathered soils. In: Bünemann E, Oberson A, Frossard E, eds. *Phosphorus in action*. Berlin, Germany: Springer, 339–369.

Reichert T, Ramming A, Fuchsleuger L, Lugli LF, Quesada CA, Fleisher K. 2022. Plant phosporus-use and -acquisition strategies in Amazonia. *New Phytologist* **234**: 1126–1143.

Sarmiento C, Zalamea P-C, Dalling JW, Davis AS, Stump SM, U'Ren JM, Arnold AE. 2017. Soilborne fungi have host affinity and host-specific effects on seed germination and survival in a lowland tropical forest. *Proceedings of the National Academy of Sciences, USA* **114**: 11458–11463.

Segnitz RM, Russo SE, Davies SJ, Peay KG. 2020. Ectomycorrhizal fungi drive positive phylogenetic plant–soil feedbacks in a regionally dominant tropical plant family. *Ecology* **101**: e03083.

Shannon CE. 1948. A mathematical theory of communication. *The Bell System Technical Journal* **27**: 379–423.

Smith ME, Henkel TW, Catherine Aime M, Fremier AK, Vilgalys R. 2011. Ectomycorrhizal fungal diversity and community structure on three co-occurring leguminous canopy tree species in a Neotropical rainforest. *New Phytologist* **192**: 699–712.

Smith SE, Read DJ. 2008. *Mycorrhizal symbiosis, 3rd edn*. London, UK: Academic Press.

Song H, Singh D, Tomlinson KW, Yang X, Ogwu MC, Slik JWF, Adams JM. 2019. Tropical forest conversion to rubber plantation in southwest China results in lower fungal beta diversity and reduced network complexity. *FEMS Microbiology Ecology* **95**: fiz092.

Sørensen TJ. 1948. A method of establishing groups of equal amplitude in plant sociology based on similarity of species content and its application to analyses of the vegetation on Danish commons. *Biologiske Skrifter* **5**: 1–34.

Sterkenburg E, Bahr A, Brandström Durling M, Clemmensen KE, Lindahl BD. 2015. Changes in fungal communities along a boreal forest soil fertility gradient. *New Phytologist* **207**: 1145–1158.

Strullu-Derrien C, Kenrick P, Selosse MA. 2016. Origins of the mycorrhizal symbioses. In: Martin FM, ed. *Molecular mycorrhizal symbiosis*. Hoboken, NJ, USA: Wiley-Blackwell, 1–20.

Tedersoo L, Bahram M, Põlme S, Kõljalg U, Yorou NS, Wijesundera R, Ruiz LV, Vasco-Palacios AM, Thu PQ, Suija A *et al.* 2014. Global diversity and geography of soil fungi. *Science* **346**: 1256688.

Tedersoo L, Bahram M, Toots M, Diedhiou AG, Henkel TW, Kjøller R, Morris MH, Nara K, Nouhra E, Peay KG. 2012. Towards global patterns in the diversity and community structure of ectomycorrhizal fungi. *Molecular Ecology* **21**: 4160–4170.

Tedersoo L, May TW, Smith ME. 2010a. Ectomycorrhizal lifestyle in fungi: global diversity. distribution and evolution of phylogenetic lineages. *Mycorrhiza* **20**: 214–263.

Tedersoo L, Sadam A, Zambrano M, Valencia R, Bahram M. 2010b. Low diversity and high host preference of ectomycorrhizal fungi in Western Amazonia, a neotropical biodiversity hotspot. *The ISME Journal* **4**: 465–471.

Tedersoo L, Smith ME. 2013. Lineages of ectomycorrhizal fungi revisited: foraging strategies and novel lineages revealed by sequences from belowground. *Fungal Biology Reviews* **27**: 83–99.

Ter Braak CJ. 1994. Canonical community ordination. Part I: Basic theory and linear methods. *Ecoscience* **1**: 127–140.

Toju H, Sato H, Tanabe AS. 2014. Diversity and spatial structure of belowground plant–fungal symbiosis in a mixed subtropical forest of ectomycorrhizal and arbuscular mycorrhizal plants. *PLoS ONE* **9**: e86566.

Turner BL, Condron LM, Richardson SJ, Peltzer DA, Allison VJ. 2007. Soil organic phosphorus transformations during pedogenesis. *Ecosystems* **10**: 1166–1181.

Valverde-Barrantes OJ, Freschet GT, Roumet C, Blackwood CB. 2017. A worldview of root traits: the influence of ancestry, growth form, climate and mycorrhizal association on the functional trait variation of fine-root tissues in seed plants. *New Phytologist* **215**: 1562–1573.

Vandepol N, Liber J, Desirò A, Na H, Kennedy M, Barry K, Grigoriev IV, Miller AN, O'Donnell K, Stajich JE, Bonito G. 2020. Resolving the Mortierellaceae phylogeny through synthesis of multi-gene phylogenetics and phylogenomics. *Fungal Diversity* **104**: 267–289.

Vasco-Palacios AM, Bahram M, Boekhout T, Tedersoo L. 2020. Carbon content and pH as important drivers of fungal community structure in three Amazon forests. *Plant and Soil* **450**: 11–131.

Vitousek PM, Sanford RL Jr. 1986. Nutrient cycling in moist tropical forest. *Annual Review of Ecology and Systematics* **17**: 137–167.

Walker T, Syers JK. 1976. The fate of phosphorus during pedogenesis. *Geoderma* **15**: 1–19.

Weemstra M, Peay KG, Davies SJ, Mohamad M, Itoh A, Tan S, Russo SE. 2020. Lithological constraints on resource economies shape the mycorrhizal composition of a Bornean rain forest. *New Phytologist* **228**: 253–268.

White TJ, Bruns T, Lee S, Taylor JW. 1990. Amplification and direct sequencing of fungal ribosomal RNA genes for phylogenetics. In: Innis MA, Gelfand DH, Sninsky JJ, White TJ, eds. *PCR protocols: a guide to the methods and applications*. London, UK: Academic Press, 315–322.

Wood SN. 2011. Fast stable restricted maximum likelihood and marginal likelihood estimation of semiparametric generalized linear models. *Journal of the Royal Statistical Society: Series B (Statistical Methodology)* **73**: 3–36.

Wu Q-S, Li GH, Ying-Ning Z. 2011. Roles of arbuscular mycorrhizal fungi on growth and nutrient acquisition of peach (*Prunus persica* L. Batsch) seedlings. *Journal of Animal and Plant Sciences* **21**: 746–750.

Xia M, Valverde-Barrantes OJ, Suseela V, Blackwood CB, Tharayil N. 2021. Coordination between compound-specific chemistry and morphology in plant roots aligns with the ancestral mycorrhizal association in woody angiosperms. *New Phytologist* **232**: 1259–1271.

Yan H, Freschet GT, Wang H, Hogan JA, Li S, Valverde-Barrantes OJ, Fu X, Wang R, Dai X, Jiang L *et al.* 2022. Mycorrhizal symbioses pathway and edaphic fertility frame root economics space among tree species. *New Phytologist* **234**: 1639–1653.

Supporting Information

Additional Supporting Information may be found online in the Supporting Information section at the end of the article.

Fig. S1 Relationship between remaining root system fresh mass and dry mass for harvested entire root systems.

Fig. S2 Graphical depiction of root processing methods.

Fig. S3 Principal components analyses for 11 root functional traits and 14 tissue elemental concentrations from root systems from 150 tropical trees.

Fig. S4 Fungal Shannon's diversity (H') and its relationship with forward-selected environmental variables.

Fig. S5 Fungal species richness in relation to forward-selected environmental variables.

Fig. S6 Fungal evenness in relation to forward-selected environmental variables.

Fig. S7 Percent of variation explained by constrained and unconstrained db-RDA axes.

Fig. S8 Constrained ordination contour plots of fitted GAM model surfaces for non-forward-selected soil variables.

Fig. S9 Constrained ordination contour plots of fitted GAM model surfaces for non-forward-selected root functional traits.

Fig. S10 Constrained ordination contour plots of fitted GAM model surfaces for non-forward-selected root tissue elemental concentrations.

Fig. S11 Percent of relative abundance (ITS2 OTU read counts) for 20 fungi species that drove Sørensen dissimilarity among root-associated fungal communities of 150 trees across 3 plots in Xishuangbanna, China.

Fig. S12 Absolute and relative abundance of ITS2 sequence reads per FunGuild fungal guild classification for 150 root systems collected in three plots in Xishuangbanna, Yunnan, China.

Fig. S13 Absolute and relative abundance of ITS2 sequence reads per FunGuild fungal guild classification for ECM-host trees.

Fig. S14 Least-squares means (±95% confidence intervals) for four root functional traits which were forward selected for the db-RDA analysis.

Methods S1 Environment of the study plots in Xishuangbanna, China.

Methods S2 Details on soil measurements.

Methods S3 Details on measurements of root tissue elemental concentrations.

Methods S4 Detailed methods for root sample processing, DNA extraction, and PCR amplification.

Methods S5 The FUNGuild database and details about the fungal guild classification reduction.

Methods S6 Details regarding the forward selection of variables.

Methods S7 Methodological details on hierarchical variation partitioning.

Table S1 Primer sequences used in DNA amplification.

Table S2 Forward selection of variables on Hellinger-transformed fungal OTU read count matrix 150 root systems sampled across three plots in Xishuangbanna, China.

Table S3 Contributions of root functional traits to the first three Principal Component axes of the root functional trait space.

Table S4 Contributions of root elemental concentrations to the first three Principal Component axes of the root functional trait space.

Table S5 Linear regression summaries for the relationships of forward-selected environmental variables and species richness, Shannon's Diversity (H'), and evenness of root-associate fungal community.

Table S6 Statistical significance of db-RDA terms.

Table S7 Model parameters for generalized additive models (GAMs) fitted to non-forward selected soils variables of the first two axes of the db-RDA.

Table S8 Model parameters for generalized additive models (GAMs) fitted to non-forward root function traits of the first two axes of the db-RDA.

Table S9 Model parameters for generalized additive models (GAMs) fitted to non-forward root tissue elemental concentrations of the first two axes of the db-RDA.

Table S10 ANOVA statistics for linear models of root functional traits by site.

Please note: Wiley is not responsible for the content or functionality of any Supporting Information supplied by the authors. Any queries (other than missing material) should be directed to the *New Phytologist* Central Office.